

## Supplemental Information

### Impact of Sodium Vanadium Oxide ( $\text{NaV}_3\text{O}_8$ , NVO) Material Synthesis Conditions on Charge Storage Mechanism in Zn-ion Aqueous Batteries

<sup>†</sup>Christopher R. Tang<sup>1,2</sup>, <sup>‡</sup>Gurpreet Singh<sup>1,3</sup>, <sup>‡</sup>Lisa M. Housel<sup>1,4</sup>, Sung Joo Kim<sup>4,5</sup>, Calvin D. Quilty<sup>1,3</sup>, Yimei Zhu<sup>4,5</sup>, Lei Wang<sup>1,4</sup>, Kenneth J. Takeuchi<sup>1,3\*</sup>, Esther S. Takeuchi<sup>1,2,3,4\*</sup>, Amy C. Marschilok<sup>1,2,3,4\*</sup>

<sup>1</sup>Institute for Electrochemically Stored Energy, State University of New York at Stony Brook, Stony Brook, New York 11794, United States

<sup>2</sup>Department of Materials Science and Chemical Engineering, Stony Brook University, Stony Brook, New York 11794, United States

<sup>3</sup>Department of Chemistry, Stony Brook University, Stony Brook, New York 11794, United States

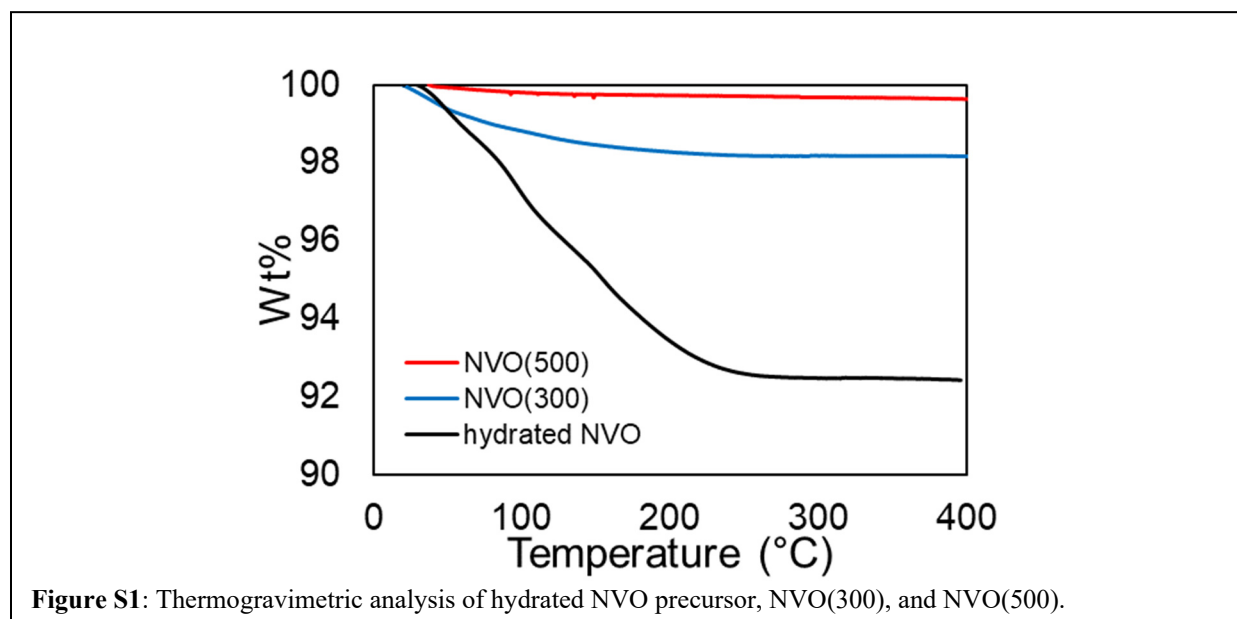
<sup>4</sup>Interdisciplinary Science Department, Brookhaven National Laboratory, Upton, New York 11973, United States

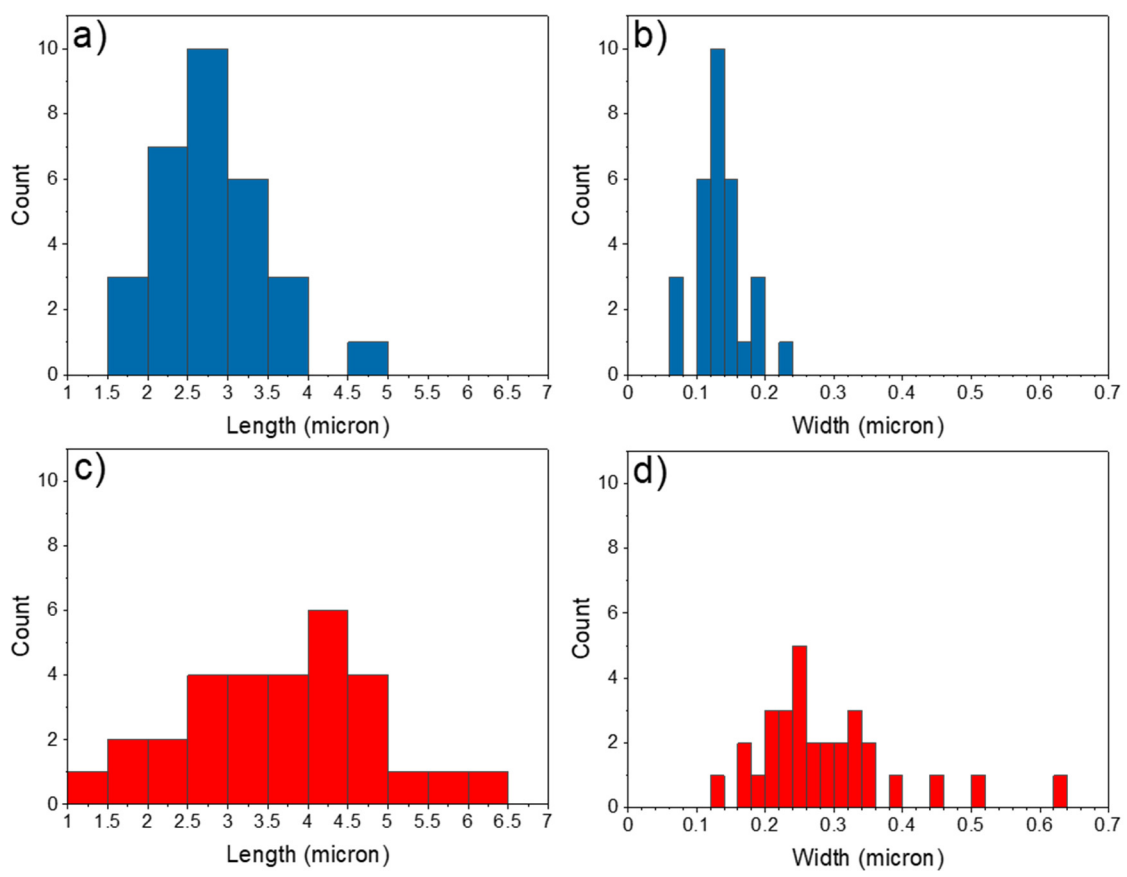
<sup>5</sup>Condensed Matter Physics and Materials Science Department, Brookhaven National Laboratory, Upton, New York 11973, United States

<sup>6</sup>Department of Physics and Astronomy, Stony Brook University, Stony Brook, New York 11794, United States

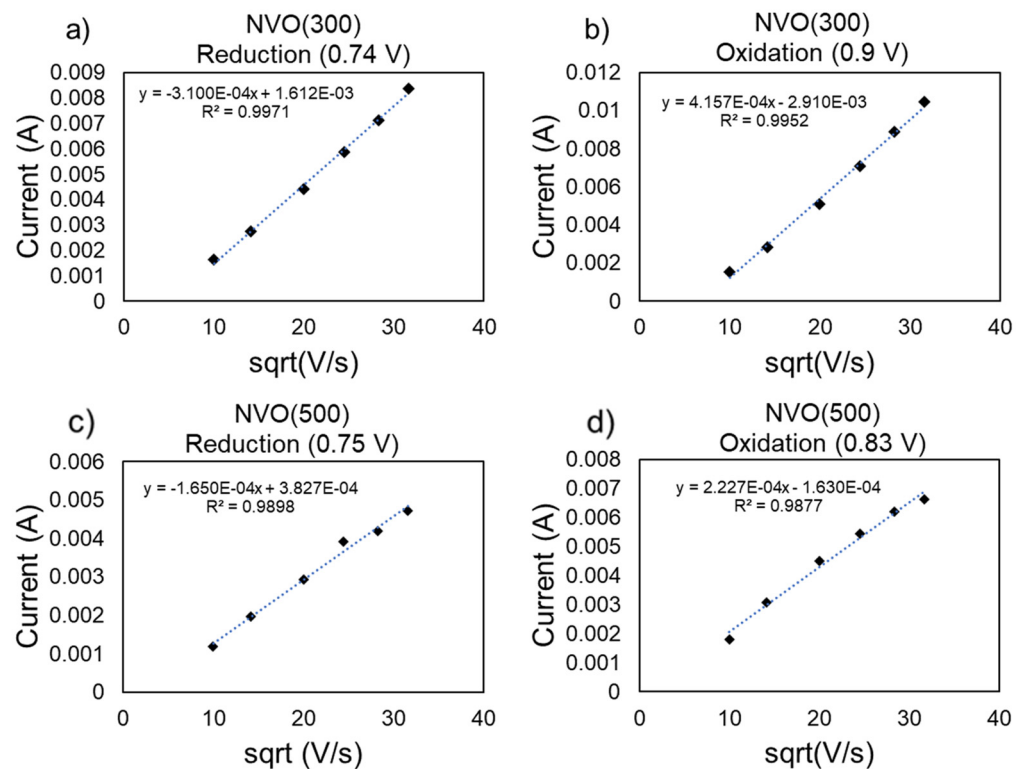
<sup>†</sup>contributed equally to the manuscript

\*corresponding authors: (K.J.T.) [kenneth.takeuchi.1@stonybrook.edu](mailto:kenneth.takeuchi.1@stonybrook.edu), (E.S.T.) [esther.takeuchi@stonybrook.edu](mailto:esther.takeuchi@stonybrook.edu), (A.C.M.) [amy.marschilok@stonybrook.edu](mailto:amy.marschilok@stonybrook.edu)

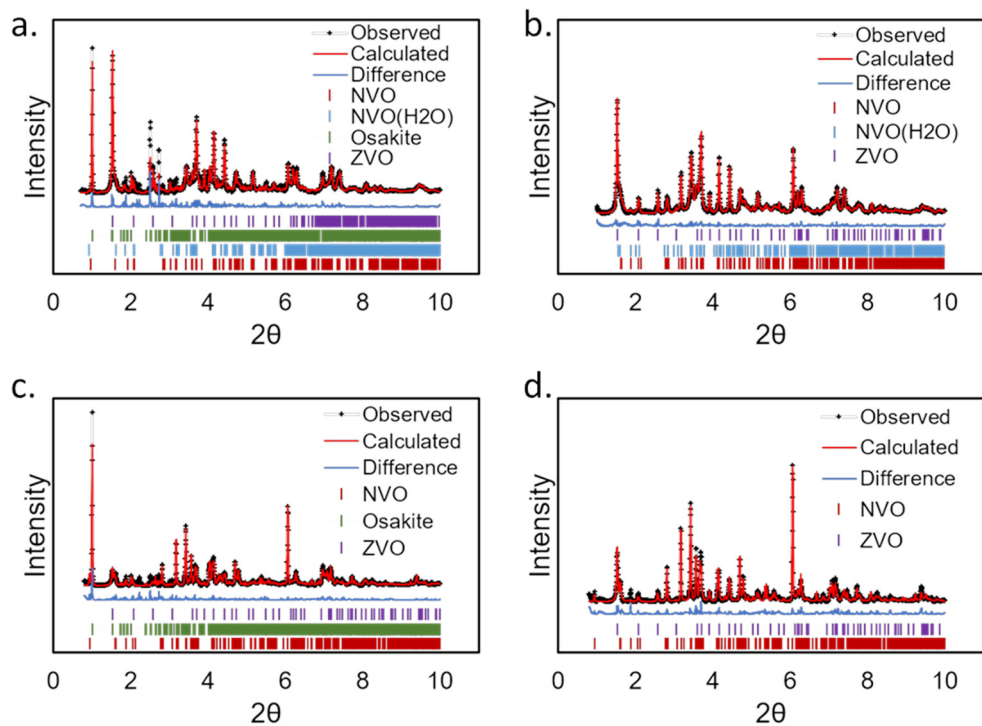




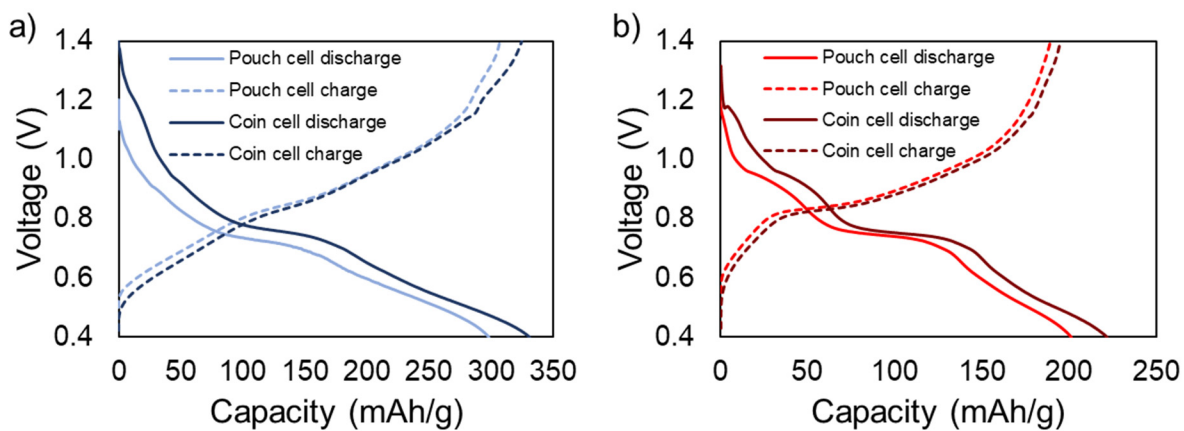
**Figure S2.** Particle size analysis of SEM image data for **a.** NVO(300) length **b.** NVO(300) width **c.** NVO(500) length and **d.** NVO(500) width.



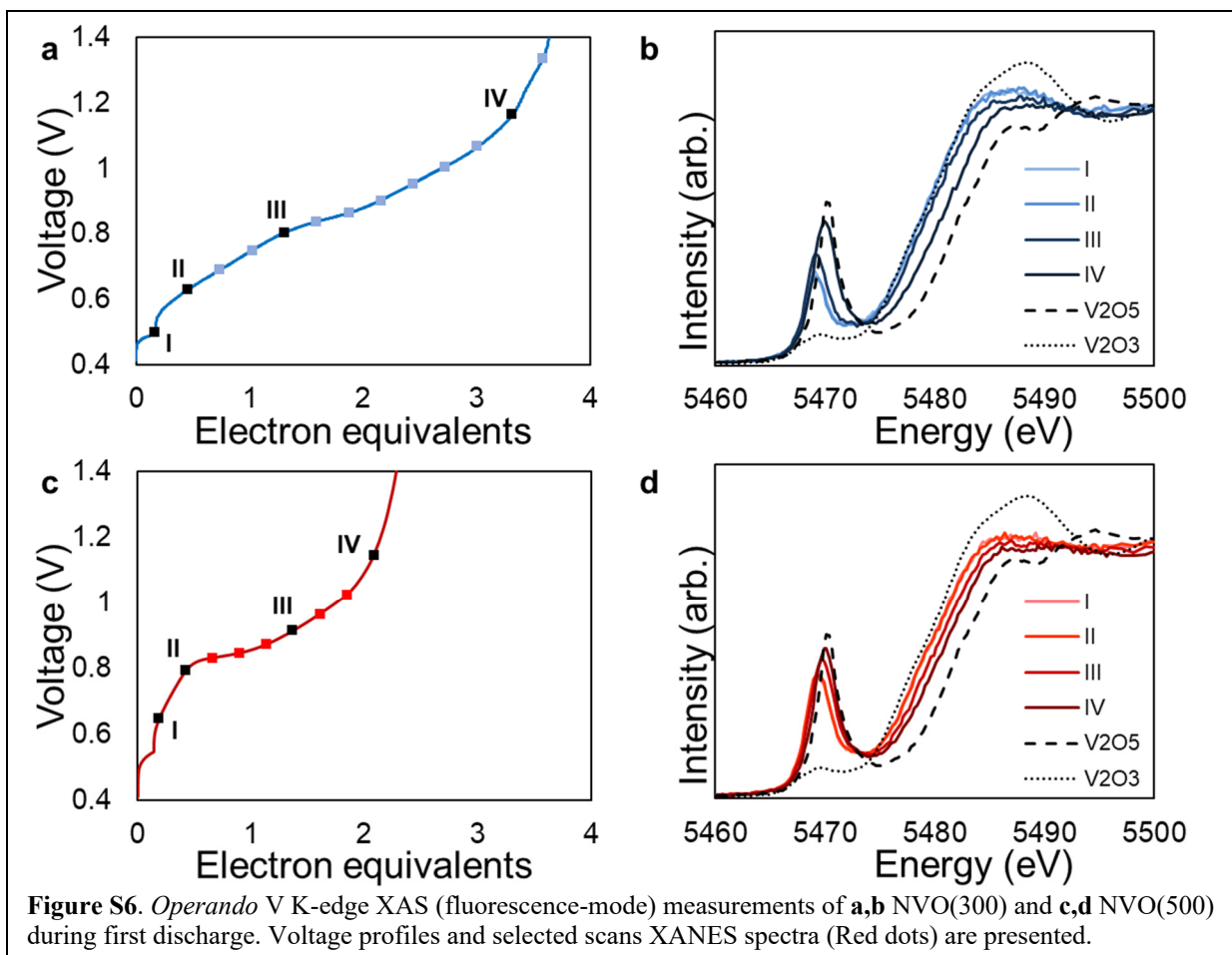
**Figure S3.** Peak current vs. the square root of the scan rate for **a,b** NVO(300) and NVO(500). All peak currents show linear responses to the change in scan rate, indicating free diffusion of the redox species to the electrode.



**Figure S4.** XRD patterns and Rietveld refinements of **a, b)** NVO(300) and **c,d)** NVO(500) electrodes after **a, c)** discharge to 0.4 V and **b, d)** charge to 1.4 V at 50 mA/g.



**Figure S5.** First cycle discharge and charge for *operando* cell and *ex situ* cell for **a)** NVO(300) and **b)** NVO(500)



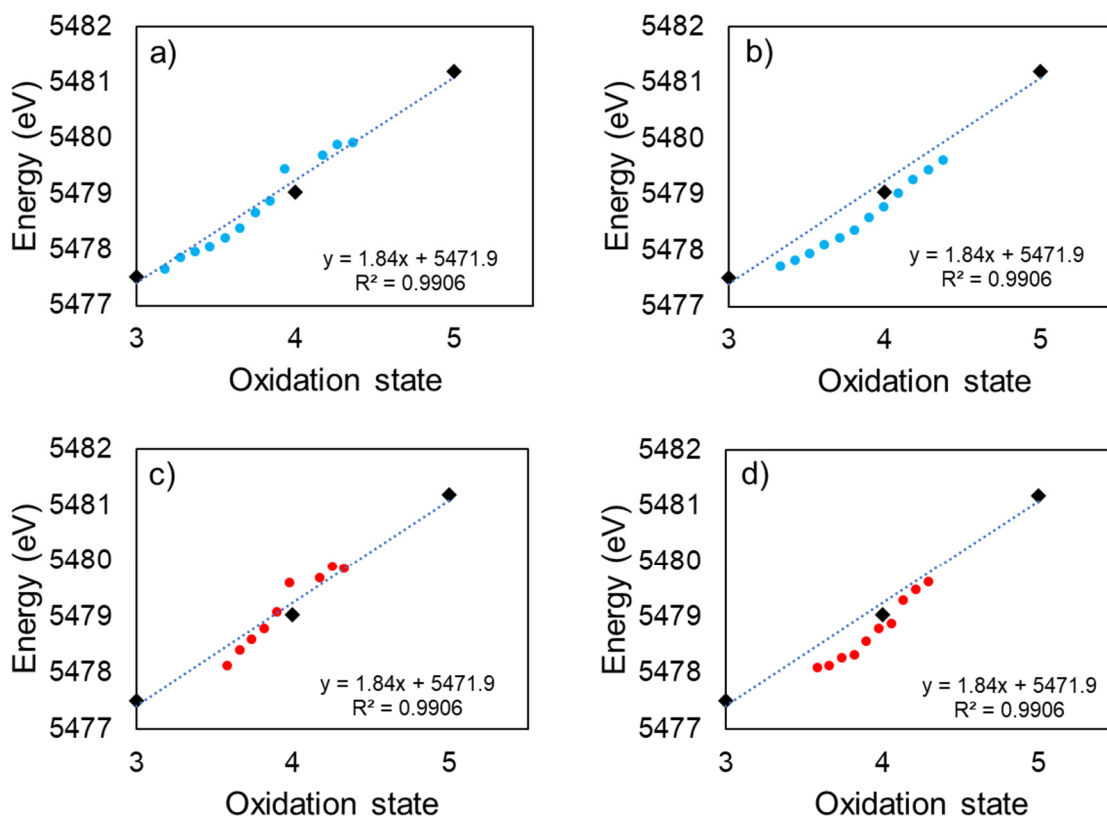


**Figure S7.** Change edge energy of *operando* XAS of NVO(300) cell during **a.** discharge and **b.** charge. Change edge energy of *operando* XAS of NVO(500) cell during **c.** discharge and **d.** charge.  $V_2O_3$ ,  $VO_4$ , and  $V_2O_5$  edge energies are shown as red dots for oxidation states  $V^{3+}$ ,  $V^{4+}$ , and  $V^{5+}$ , respectively.

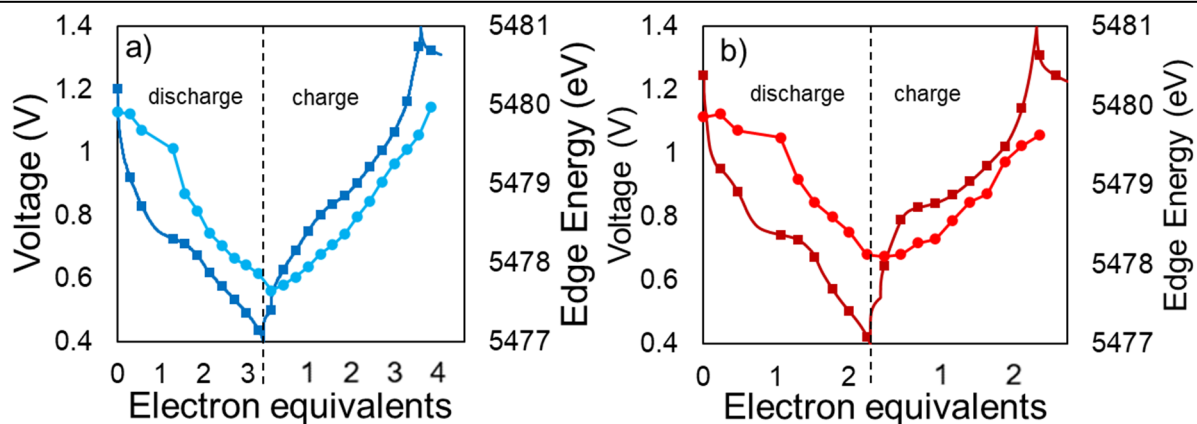


**Figure S8.** V K-edge position during cycle of **a.** NVO(300) and **b.** NVO(500) *operando* cells. Voltage profiles are denoted with square symbols. Edge position is denoted with circle symbols

**Table S1.** Rietveld refinement parameters of NVO(300) and NVO(500) powders.

Parameter	NVO(300)	NVO(500)
	Anhydrous/Monohydrate	
Space Group	P <sub>21</sub> /m	P <sub>21</sub> /m
Phase Composition	23(1) %/76(1) %	100 %
a (Å)	7.43(1) Å/7.221(5) Å	7.295(1) Å
b (Å)	3.620(1) Å/3.6134(4) Å	3.6109(2) Å
c (Å)	12.10(3) Å/12.20(1) Å	12.18(1) Å
α (°)	90.0 °/90.0 °	90.0 °
β (°)	106.85(5) °/107.66(2) °	107.77(1) °
γ (°)	90.0 °/90 °	90.0 °
V (Å <sup>3</sup> )	311.8(2) Å <sup>3</sup> /303.4(1) Å <sup>3</sup>	305.55(4) Å <sup>3</sup>
Crystallite Size (Axial, nm)	0.0193(6) μm/0.0167(4) μm	0.061(1) μm
Crystallite Size (equatorial, nm)	1.0 μm/1.0 μm	1.0 μm
microstrain (%)	0.12(1) %/0.07(3) %	0.02(1) %
%R <sub>wp</sub>	5.99 %	8.26 %

**Table S2.** Refined atomic positions of NVO(300) powder.

Atom	X	Y	Z
	Anhydrous/Monohydrate	Anhydrous/Monohydrate	Anhydrous/Monohydrate
V1	0.897(4)/0.877(3)	0.250/0.250	0.545(5)/0.548(1)
V2	0.161(4)/0.204(2)	0.250/0.250	0.100(4) /0.0837(9)
V3	0.024(5)/0.075(2)	0.250/0.250	0.797(4)/0.815(1)
O1	0.01(1)/0.0213(7)	0.250/0.250	0.42(2)/0.436(6)
O2	0.82(1)/0.73(1)	0.250/0.250	0.87(2)/0.89(4)
O3	0.79(2)/0.842(7)	0.250/0.250	0.64(1)/0.669(4)
O4	0.15(1)/0.428(8)	0.250/0.250	0.26(1)/0.189(4)
O5	0.58(1)/0.624(9)	0.250/0.250	0.56(1)/0.440(4)
O6	0.24(1)/0.307(6)	0.250/0.250	0.94(1)/0.960(3)
O7	0.30(1)/0.248(8)	0.250/0.250	0.80(1)/0.739(4)
O8	1.03(1)/1.01(1)	0.250/0.250	0.19(2)/0.184(4)
Na1	0.42(1)/0.48(1)	0.250/0.250	0.66(1)/0.672(5)
Na2	0.568/0.574(4)	0.250/0.250	0.059/0.038(5)
O <sub>H2O</sub>	---/0.537(8)	---/0.250	---/0.352(3)

**Table S3.** Refined atomic positions of NVO(500) powder.

Atom	X	Y	Z
V1	0.857(1)	0.250	0.5453(7)
V2	0.181(1)	0.250	0.0806(6)
V3	0.075(1)	0.250	0.8132(6)
O1	0.069(3)	0.250	0.451(2)
O2	0.889(3)	0.250	0.925(2)
O3	0.816(3)	0.250	0.678(2)
O4	0.371(3)	0.250	0.191(2)
O5	0.632(4)	0.250	0.452(2)
O6	0.270(3)	0.250	0.965(2)
O7	0.229(3)	0.250	0.737(2)
O8	1.000(4)	0.250	0.169(2)
Na1	0.500(2)	0.250	0.669(1)
Na2	0.586	0.250	0.059

**Table S4.** Cathodic and anodic peak values,  $\Delta E$  values, and  $E_{1/2}$  values at the different scan rates for CV of NVO(300).

Redox Couple	Scan Rate (mV/s)	Cathodic Peak (V)	Anodic peak (V)	$\Delta E$ (V)	$E_{1/2}$ (V)
1	0.1	0.884	1.020	0.136	0.952
	0.2	0.872	1.030	0.158	0.951
	0.4	0.856	1.051	0.195	0.954
	0.6	0.838	1.082	0.244	0.96
	0.8	0.820	1.113	0.293	0.967
	1	0.810	1.142	0.332	0.976
2	0.1	0.740	0.886	0.146	0.813
	0.2	0.714	0.912	0.198	0.813
	0.4	0.682	0.957	0.275	0.8195
	0.6	0.658	0.994	0.336	0.826
	0.8	0.630	1.031	0.401	0.8305
	1	0.605	1.056	0.450	0.831

**Table S5.** Cathodic and anodic peak values,  $\Delta E$  values, and  $E_{1/2}$  values at the different scan rates for CV of NVO(500).

Redox Couple	Scan Rate (mV/s)	Cathodic Peak (V)	Anodic peak (V)	$\Delta E$ (V)	$E_{1/2}$ (V)
1	0.1	0.953	0.984	0.031	0.969
	0.2	0.940	0.998	0.058	0.969
	0.4	0.923	1.017	0.094	0.97
	0.6	0.915	1.042	0.127	0.979
	0.8	0.909	1.050	0.141	0.980
	1	0.905	1.065	0.16	0.985
2	0.1	0.731	0.885	0.150	0.81
	0.2	0.716	0.906	0.190	0.811
	0.4	0.698	0.931	0.230	0.819
	0.6	0.688	0.953	0.260	0.822
	0.8	0.676	0.967	0.291	0.8215
	1	0.670	0.980	0.306	0.827

**Table S6.** Rietveld refinement parameters of an NVO(300) electrode following discharge at 50 mA/g to 0.4 V.

Parameter	NVO(300)	NVO(300)	ZHS	ZVO
	Anhydrous	Monohydrate		
Space Group	P2 <sub>1</sub> /m	P2 <sub>1</sub> /m	P-1	P-3/m1
Phase Composition	26(7) %	22(5) %	16(1) %	36(1) %
a (Å)	7.26(7) Å	7.11(8) Å	8.328(9) Å	6.109(1) Å
b (Å)	3.620(1) Å	3.612(3) Å	8.323(9) Å	6.109(1) Å
c (Å)	12.0(1) Å	12.3(2) Å	10.987(6) Å	7.160(2) Å
α (°)	90.0°	90.0°	94.05(4)°	90.0°
β (°)	108.0(3)°	105.8(3)°	83.32(3)°	90.0°

**Table S7.** Rietveld refinement parameters of an NVO(300) electrode following discharge to 0.4 V and charge to 1.4 V at 50 mA/g.

Parameter	NVO(300)	NVO(300)	ZVO
	Anhydrous	Monohydrate	
Space Group	P2 <sub>1</sub> /m	P2 <sub>1</sub> /m	P-3/m1
Phase Composition	61(1) %	13(1) %	26.2(4) %
a (Å)	7.05(1) Å	7.328(8) Å	6.0884(9) Å
b (Å)	3.6138(2) Å	3.600(1) Å	6.0884(9) Å
c (Å)	12.32(3) Å	12.37(3) Å	7.1798(9) Å
α (°)	90.0°	90.0°	90.0°
β (°)	108.34(5)°	109.57(4)°	90.0°

**Table S8.** Rietveld refinement parameters of NVO(500) electrode after discharge at 50 mA/g to 0.4 V.

Parameter	NVO(500)	ZHS	ZVO
Space Group	P2 <sub>1</sub> /m	P-1	P-3/m1
Phase Composition	62(1) %	25.4(8) %	12.3(8) %
a (Å)	7.156(7) Å	8.355(6) Å	6.125(5) Å
b (Å)	3.6245(2) Å	8.356(6) Å	6.125(5) Å
c (Å)	12.34(1) Å	11.006(6) Å	7.151(4) Å
$\alpha$ (°)	90.0°	94.27(3)°	90.0°
$\beta$ (°)	108.44(2)°	83.06(3)°	90.0°

**Table S9.** Rietveld refinement parameters of NVO(500) electrode after discharge to 0.4 V and charge to 1.4 V at 50 mA/g.

Parameter	NVO(500)	ZVO
Space Group	P2 <sub>1</sub> /m	P-3/m1
Phase Composition	76.6(9) %	23.4(6) %
a (Å)	7.151(6) Å	6.105(2) Å
b (Å)	3.6254(2) Å	6.105(2) Å
c (Å)	12.35(1) Å	7.187(2) Å
$\alpha$ (°)	90.0°	90.0°
$\beta$ (°)	108.43(2)°	90.0°